

RESEARCH

Open Access



ERMAP attenuates DSS-induced colitis in mice by regulating macrophage and T cell functions

Lu Xia^{1,2,3†}, Yiwen Pan^{2†}, Xianbin Wang², Rong Hu⁴, Jie Gao⁴, Wei Chen², Keke He², Dongbin Cui¹, Youbo Zhao¹, Lu Liu^{5*}, Lijun Lai^{6*} and Min Su^{1,2,3,7*}

Abstract

Background & aims Both macrophages and T cells play a critical role in inflammatory bowel disease (IBD) development. Since our previous studies have shown that a novel immune checkpoint molecule erythrocyte membrane-associated protein (ERMAP) affects macrophage polarization and negatively regulates T cell responses, we investigated the effects of ERMAP on DSS-induced colitis progression in mice.

Methods C57BL/6 mice developed a dextran sodium sulfate (DSS) colitis model, treated with control Fc protein (Control Ig) and ERMAP-Fc fusion protein (ERMAP-Ig) for 12 days to assess colitis severity by disease activity index (DAI), weight loss, colon length, histology, flow cytometry, Q-PCR, WB, ELISA, and the effect of adoptive transfer of ERMAP knockout mice (ERMAP^{-/-}) peritoneal macrophages on DSS colitis mice. In vitro, the effects of the RAW264.7 macrophage cell line that interfered with ERMAP expression on macrophage polarization and T cells were analyzed by flow cytometry.

Results We show here that administration of ERMAP protein significantly increases the proportion of anti-inflammatory M2-type macrophages and inhibits T cell activation and proliferation in DSS-induced colitis mice. Knockdown of ERMAP in RAW264.7 macrophages reduces M2-type macrophage polarization and increases T cell responses. Adoptive transfer of macrophages from ERMAP^{-/-} exacerbates DSS-induced colitis. Global gene expression analysis by RNA-seq shows that ERMAP inhibits the NOD-like receptor (NLR) protein family pathway in macrophages.

Conclusions In summary, our results suggest that administration of ERMAP can protect DSS-induced colitis in mice by regulating T cell and macrophage functions. This study adds to the evidence for various mechanistic pathways associated to the pathogenesis of IBD, which could subsequently be translated to novel therapeutics.

[†]Lu Xia and Yiwen Pan contributed equally to this work.

*Correspondence:

Lu Liu
2501336721@qq.com
Lijun Lai
lajun.lai@uconn.edu
Min Su
sumin@gmc.edu.cn

Full list of author information is available at the end of the article



Key messages

Administration of ERMAP protein ameliorates DSS-induced colitis in mice by inhibiting T cell activation and proliferation and enhancing M2-type macrophage polarization.

Keywords ERMAP, Inflammatory bowel disease, Macrophages, T cells

Introduction

Inflammatory bowel disease (IBD) is a group of disorders that are characterized by chronic inflammation of the gastrointestinal (GI) tract [1]. IBD includes Crohn's disease and ulcerative colitis. Both T cells and macrophages play a critical role in the pathogenesis of IBD [2].

Specifically, CD4⁺ T cell subsets exhibit distinct pro-inflammatory profiles in IBD. In Crohn's disease, lamina propria CD4⁺ T cells predominantly secrete Th1/Th17-associated cytokines (such as TNF- α , IFN- γ , IL-17A). In ulcerative colitis, CD4⁺ T cells can secrete a large number of Th2 effect-related inflammatory factors (such as IL-4, IL-13) and Th17 related pro-inflammatory cytokines (IL-17A). These T cell-derived cytokines not only directly damage intestinal tissue but also stimulate macrophage polarization.

Intestinal macrophages originating from circulating monocytes in the blood or intestinal resident macrophages pools are important immune cells against foreign pathogens [3, 4]. Intestinal macrophages are situated at the interface of intestinal lumen; by identifying pathogen-associated molecular patterns (PAMPs) and damage-associated molecular patterns (DAMPs), they quickly recognize pathogens and tissue damage, and deliver signals to different immune cells to maintain environmental homeostasis in the gut [5]. Macrophages can polarize into classically activated macrophages (M1) and selectively activated macrophages (M2) [6]. M1 polarization can be induced by IFN- γ , lipopolysaccharide (LPS), and TNF- α , leading to increased production of pro-inflammatory cytokines (IL-1 β , TNF- α , and IL-6) and active oxygen. These mediators further exacerbate inflammation and tissue damage by promoting T cell differentiation and activation [7]. M2 polarization is stimulated by IL-4, IL-13 and M-CSF, resulting in decreased levels of pro-inflammatory cytokines and increased production of anti-inflammatory cytokines (IL-10, IL-4), mannose receptor (CD206) and arginase I (Arg1) [8]. The imbalance of M1 and M2 macrophages is associated with the occurrence, development and prognosis of IBD [9]. M1 macrophages are dominating in IBD and inducing inflammatory responses in advanced stages of the disease, whereas M2 macrophages have anti-inflammatory properties and are involved in tissue recovery after injury [10]. Therefore, regulating macrophage polarization could be used in the treatment of IBD.

Immune cells are regulated by immune checkpoint molecules [11]. In past several years, several new drugs that target the immune checkpoint molecules have been approved by the FDA for the treatment of autoimmune disease and cancer, highlighting the importance of these molecules. For example, the recombinant CTLA-4-Fc fusion protein has been used to treat rheumatoid arthritis and kidney graft rejection [12]. In contrast, antibodies against PD-L1/PD-1 or CTLA-4 have been used to treat a variety of cancer [13]. An increasing number of new immune checkpoint molecules are being discovered. For example, CD300c and TAPBPL have been identified as novel checkpoint molecules that can inhibit T cell functions in vitro and in vivo [14, 15].

Erythrocyte Membrane-associated Protein (ERMAP) is also a new checkpoint molecule containing both an extracellular immunoglobulin domain and an intracellular B30.2 domain [16, 17]. ERMAP shares sequence and structural similarities with the existing immune checkpoint molecules [17, 18]. It has been shown that ERMAP can enhance the generation of M2 macrophages and inhibit T cell functions in vitro [18]. Administration of ERMAP protein can ameliorate experimental autoimmune encephalomyelitis (EAE) and type I diabetes mellitus (T1D) by inhibiting auto-reactive T cell proliferation and activation and regulating macrophage polarization toward M2 [18].

In this study, we investigated the effects of ERMAP on dextran sodium sulfate (DSS)-induced colitis and found that administration of ERMAP-Fc fusion protein (ERMAP-Ig) effectively protected DSS-induced colitis as compared to control Fc protein (Control Ig) treatment. In contrast, adoptive transfer of macrophages from ERMAP gene knockout mice exacerbated DSS-induced colitis.

Materials and methods

Cloning and purification of ERMAP-Ig

The extracellular domain of hERMAP (aa30-145) was cloned and fused into a pCMV6- AC-FC-S expression vector containing the constant region of mouse IgG2a (ORIGENE, Rockville, MD). Vectors were transfected into HEK-293 cells, and ERMAP-Ig in the supernatant was purified by the protein purification apparatus (AKTA pure, Sweden). The purity was determined by Western Blot and Coomassie blue staining and protein quantification was performed using the BCA protein detection kit (Beyotime Biotech, China) and function verified by FACS (Supplemental Fig. 1). The endotoxin levels of the

recombinant proteins were <0.01 EU/ml μg^{-1} . Control Ig (recombinant mouse IgG2a) was purchased from BioX-Cell (West Lebanon, NH).

Mice and DSS-induced colitis

C57BL/6 mice were purchased from Tianqin Biotech Co., Ltd (Hunan, China). ERMAP^{-/-} mice were generated by Shanghai Bangyao Biotechnology Co., Ltd. Stable whole-body knockout mice were selected (Supplemental Fig. 2). The mice were housed in specific pathogen-free rooms and used following a protocol approved by the Institutional Animal Care and Use Committee of Guizhou Medical University (NO: 1900035). Eight to ten-week-old C57BL/6 wild-type (WT) mice were fed with 3% Dextran sodium sulfate (DSS, 36–50 kDa, YEASEN, China) for 7 days. The mice were injected intraperitoneally (i.p.) with control Ig or ERMAP-Ig on days 3, 6, and 9 and measured for Disease activity index (DAI) scores daily. The criteria for the DAI scoring are shown in Supplemental Table 1 as described [19]. Mice were euthanized on day 12, and samples were collected. After referring to The ARRIVE guidelines 2.0 (<https://arriveguidelines.org/arrive-guidelines>), the method of choice for sacrifice of mice in this study was cervical dislocation. Cervical dislocation is a rapid and painless method of euthanasia in mice. The cervical vertebrae of the mouse are usually twisted rapidly by hand or tool, resulting in spinal cord injury, which causes immediate unconsciousness and cessation of respiration, and this method is only applicable to rodents weighing <200 g. The mice selected in this study weighed an average of 30 g each and were eligible for the cervical dislocation method, in addition to being eligible for humanitarian execution of animals.

Histopathological and Immunofluorescence

Mouse colons were fixed with 4% formaldehyde for 24 h. Tissues were embedded in paraffin, and sections were prepared (5 μm). The Sections were stained with hematoxylin-eosin (H&E) and observed under an Olympus SLIDEVIEW VS200 slide scanner. The criteria for the colitis pathology scores are shown in Supplemental Table 2 [19]. For immunofluorescence, sections were incubated with rat anti-CD86 antibody (1:100, Abcam) and rabbit anti-CD206 antibody (1:100, Cell Signaling) at 4 °C overnight, and then secondary antibody with Cy3-sheep anti-rat IgG and FITC-donkey anti-rabbit IgG (1:500) for 4 h at room temperature. The sections were counter-stained with DAPI and observed under a laser microscope (Olympus SpinSR10, Tokyo, Japan).

Isolation of colonic lamina propria cells

Colonic lamina propria cells were isolated as described [20] with minor modification. In brief, after washing with D-Hank's, epithelial cells were removed by 10 mM

DTT (30 min), 0.5 mM EDTA solution at 37 °C 30 min, digested in invisible tissue in collagenase I (1 mg/mL) containing 0.25 mg/mL DNase I and 2 mg/mL Dispase II, screened with a 70 μm cell filter. Percoll isolate monocytes and lymphocytes in the colon lamina propria. Cells were stained with specific antibodies and analyzed by cell flow cytometer.

Flow cytometry analysis

Single cell suspension from the spleen and colon was prepared and stained with fluorescent conjugated antibodies for direct or indirect staining. For intracellular staining, the cells were first permeabilized with a BD Cytofix/Cytoperm solution for 20 min at 4 °C. Cell activation: anti-CD4, CD8 and CD69⁺, Cell proliferation: anti-CD4, CD8 and Ki67⁺, Macrophages: anti-F4/80, MHC-II and CD206, Regulatory T cells (Tregs): anti-CD4, CD25 and Foxp3. Detection of cytokine expression was incubation for 6 h with PMA (100 ng/mL) / BFA (100 ng/mL) / Ionomycin (500 ng/mL). Flow analysis of TNF- α , IFN- γ , IL-4, and IL-17A expression in CD4⁺ cells. All antibodies were obtained from Biolegend, San Diego, CA, except MHC-II (Abcam, USA), ERMAP (R&D, USA). Data were analyzed on a FACS Celesta™ (BD, USA), and data were analyzed using FlowJo-V10 software (BD, USA).

In vitro culture and interference of RAW264.7

RAW264.7 cells were purchased from American Type Culture Collection (ATCC) and cultured in endotoxin-free Dulbecco's modified Eagle's medium (DMEM) containing 10% fetal bovine serum (FBS, Gibco). The mERMAP shRNA lentivirus used for cell transduction contains three expression constructs; each construct encodes a target-specific 19–25 nt (plus hairpin) shRNA (Supplemental Table 3). Validation of ERMAP knockdown was done by qRT-PCR, Western blot, and flow cytometry after puromycin selection (Supplemental Fig. 3). After the ERMAP knockdown, RAW264.7 cells were cultured at M1 (LPS 100 ng/mL, IFN- γ 2.5 ng/mL) and M2 (IL-4 40 ng/mL) conditions and analyzed by flow cytometry 24 h later.

RNA-seq

RNA from control RAW264.7 and ERMAP knockdown RAW264.7 cells was extracted using standard methods. Qubit2.0 Fluorometer for preliminary quantification, then Agilent 2100 bioanalyzer to detect the insert size of the library, and qRT-PCR to accurately quantify the effective concentration of the library (>2 nM) to ensure the quality of the library. Illumina sequencing was performed after pooling the different libraries. Sequenced fragments were converted into reads by CASAVA base calling. After raw data filtering, sequencing error rate checking, and GC content distribution checking, clean reads for

subsequent analysis were obtained. Use HISAT2 software to quickly and accurately align the Clean Reads with the reference genome, and obtain the positioning information of the Reads on the reference genome [21]. The feature Counts tool in the subread software was used to filter out reads with alignment quality values below 10, unpaired alignments, and alignments to multiple regions of the genome [22]. After the gene expression quantification was completed, the expression data were statistically analyzed, and the genes with significant differences in the expression levels of the samples under different states were screened. The mainstream hierarchical clustering was used to perform cluster analysis on the FPKM values of genes, the rows were normalized, and the clusterProfiler software was used to perform KEGG pathway enrichment analysis on differential gene sets, padj less than 0.05 as the threshold for significant enrichment.

SDS-PAGE and Western blot

Purified ERMAP-Ig was loaded on 10% SDS-PAGE, stained with Coomassie blue or transferred to PVDF membranes. Protein-containing membranes were incubated with an HRP-conjugated anti-mouse IgG2 antibody or anti-ERMMap antibody (Origend, China) and then with an HRP-conjugated secondary antibody. Membranes were then analyzed by Super Signal West Pico chemiluminescent Substrate (Thermo Fisher Scientific, Waltham, MA). The colon tissue was lysed by RIPA; Proteins were separated by SDS-PAGE and subjected to Western blot as above.

Quantitative real-time PCR (qRT-PCR) analysis

Total RNA from the tissue was extracted with Trizol, and cDNA was synthesized by using a reverse transcription kit (MonScript™ RTIII AII-in-One Mix with dsDNase, Monad, China). qRT-PCR (MonAmp™ SYBR Green qPCR Mix, Monad, China) was performed on a Bio-Rad machine (Thermo Fisher Scientific, Waltham, MA). GAPDH was used as the internal reference. The qRT-PCR primer sequences of the tested genes are listed in the Supplementary Information (Supplemental Table 4).

Enzyme-linked immunosorbent assay (ELISA)

Cytokines in mouse serum were analyzed using mouse IL-6 (Biolegend, San Diego, CA) and TGF- β 1 (Neobioscience, China) ELISA kits according to the manufacturer's instructions.

In vivo depletion and adoptive transfer of macrophages

Mice were injected i.p. with 100 μ L of clodronate on days -1 and -2 to deplete macrophages as described [23]. M0 of peritoneal macrophages from WT or ERMMap^{-/-} mice were transplanted into WT (1×10^6 per mouse) mice on day 0 [20]. DSS-induced colitis was induced 12 h after

macrophage transferred. DAI scores were measured daily, and samples were harvested on day 9.

Statistical analysis

Data were analyzed using the SPSS package (v. 26 for Windows, Chicago, IL). Continuous variables with normal distribution were presents as mean \pm standard deviation (SD). Mean of two continuous normally distributed variables were compared by independent samples Student's test. For the in vitro macrophage experiments, an ordinary one-way analysis of variance (ANOVA) test was used. For the DAI scores and body weight measurements, the Repeated Measures ANOVA test was used.

Results

ERMMap-Ig ameliorates DSS-induced colitis in mice

To determine the possible effect of ERMMap on DSS-induced colitis, C57BL/6 mice were fed with 3% DSS for 7 days to induce colitis. The mice were injected i.p. with 25 μ g ERMMap-Ig or Control Ig protein on days 3, 6 and 9. DAI scores were measured daily. ERMMap-Ig treatment significantly reduced DAI scores (Fig. 1A); Weight loss in ERMMap-Ig-treated mice was less than Control Ig-treated mice (Fig. 1B). ERMMap-Ig treatment also attenuated the colon length reduction (Fig. 1C-D). Histological examination revealed that control Ig-treated DSS-induced colitis mice had inflammatory cell infiltration, severe epithelial destruction and crypt loss, while these features were significantly improved in ERMMap-Ig-treated mice (Fig. 1E). Consequently, the histological scores of acute colitis in ERMMap-Ig-treated mice were significantly lower than those in Control Ig mice (Fig. 1F). The data suggest that ERMMap-Ig ameliorates the inflammatory response and histology damage in DSS-induced colitis. Interestingly, ERMMap^{-/-} mice showed more severe colon shortening and weight loss during colitis induction, and even three mice failed to survive to the end of modeling (Supplemental Fig. 4). Knockdown of endogenous ERMMap deprived the mice of the protective effect of inflammation. Having established the therapeutic effect of ERMMap-Ig on DSS-induced colitis, we next investigated its regulatory effects on immune cells.

ERMMap-Ig increases the population of colon M2-type macrophages

Macrophages play a critical role in the pathogenesis of DSS-induced colitis. Intestinal macrophages are located below the mucosal monolayer epithelium, where they exhibit functional diversity that can not only remove bacteria and foreign substances and eliminate senescent or dead cells, but also support regulatory T cells (Tregs) [24]. We therefore analyzed colon lamina propria macrophages by flow cytometry with antibodies against F4/80, MHCII, and CD206. As shown in Fig. 2A, M1-type

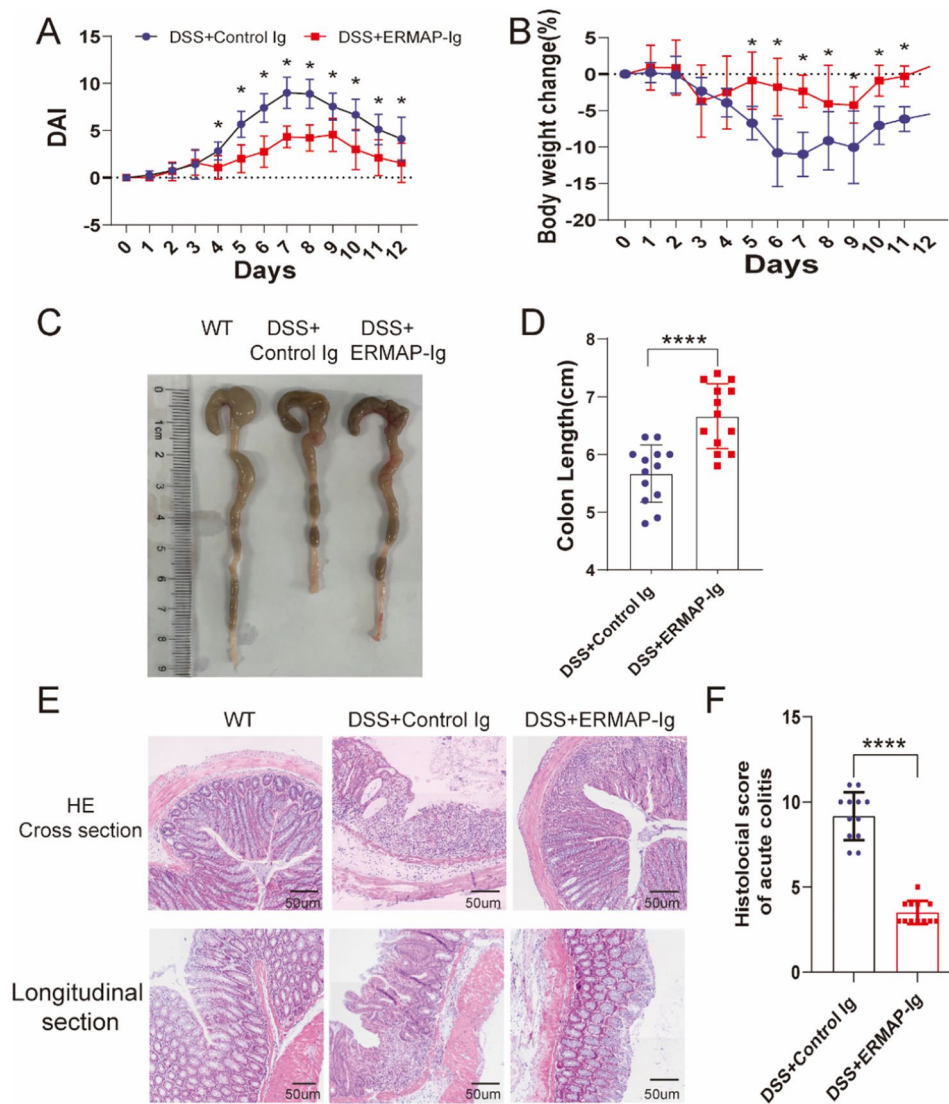


Fig. 1 ERMAP-Ig ameliorates DSS-induced colitis in mice. C57BL/6 were fed with 3% DSS for 7 days. The mice were injected i.p. with 25 μ g ERMAP-Ig or Control Ig protein on days 3, 6 and 9. **(A)** DAI scores were measured daily ($n=12$ for each group). **(B)** Weight loss was expressed as the average percentage of initial body weight \pm SEM ($n=12$ for each group). **(C-F)** The mice were euthanized on day 12. **(C)** Typical images and **(D)** statistical analysis of colon length in the Control Ig- and ERMAP-Ig-treated mice. **(E)** Representative histological HE staining images (200 \times) and **(F)** colon inflammation pathology scores. **** $P < 0.0001$ compared with DSS+Control Ig

macrophages (F4/80⁺ MHCII^{hi} CD206^{lo}) were decreased, whereas M2-type macrophages (F4/80⁺ MHCII^{lo} CD206^{hi}) were significantly increased in ERMAP-Ig mice.

CD4⁺ CD25⁺ Foxp3⁺ Tregs have been reported to play a role in ameliorating DSS-induced colitis [25]. Induction of Tregs can repair tissues, reshape the extracellular matrix, and promote epithelial cell renewal. Macrophages are unique among lamina propria APCs in their ability to promote the generation of Tregs [26]. We found that ERMAP-Ig treatment increased the percentage of Tregs in the mice (Fig. 2B), which also increased the proportion of Th2-type cells (CD4⁺ IL-4⁺ T cells) and reduced the proportion of pathogenic Th1 (CD4⁺ TNF- α ⁺ T cells and

CD4⁺ IFN- γ ⁺ T cells) and Th17(CD4⁺ IL-17A⁺ T cells) (Fig. 2E).

CD86 is a co-stimulatory factor. Our immunofluorescence staining showed that the proportion of CD86⁺ cells were significantly lower in ERMAP-Ig-treated DSS-induced colitis mice, whereas the percentage of CD206⁺ cells were higher in ERMAP-Ig-treated mice than in control Ig- treated mice (Fig. 2C). We also analyzed the expression levels of M2 and M1 macrophage-related genes. The mRNA levels of M2-related genes Arg1 and CD206 were increased in ERMAP-Ig colon tissues, whereas the expression level of M1-related gene iNOS was decreased (Fig. 2D), consistent with the data that M1 macrophages were decreased, whereas M2 macrophages

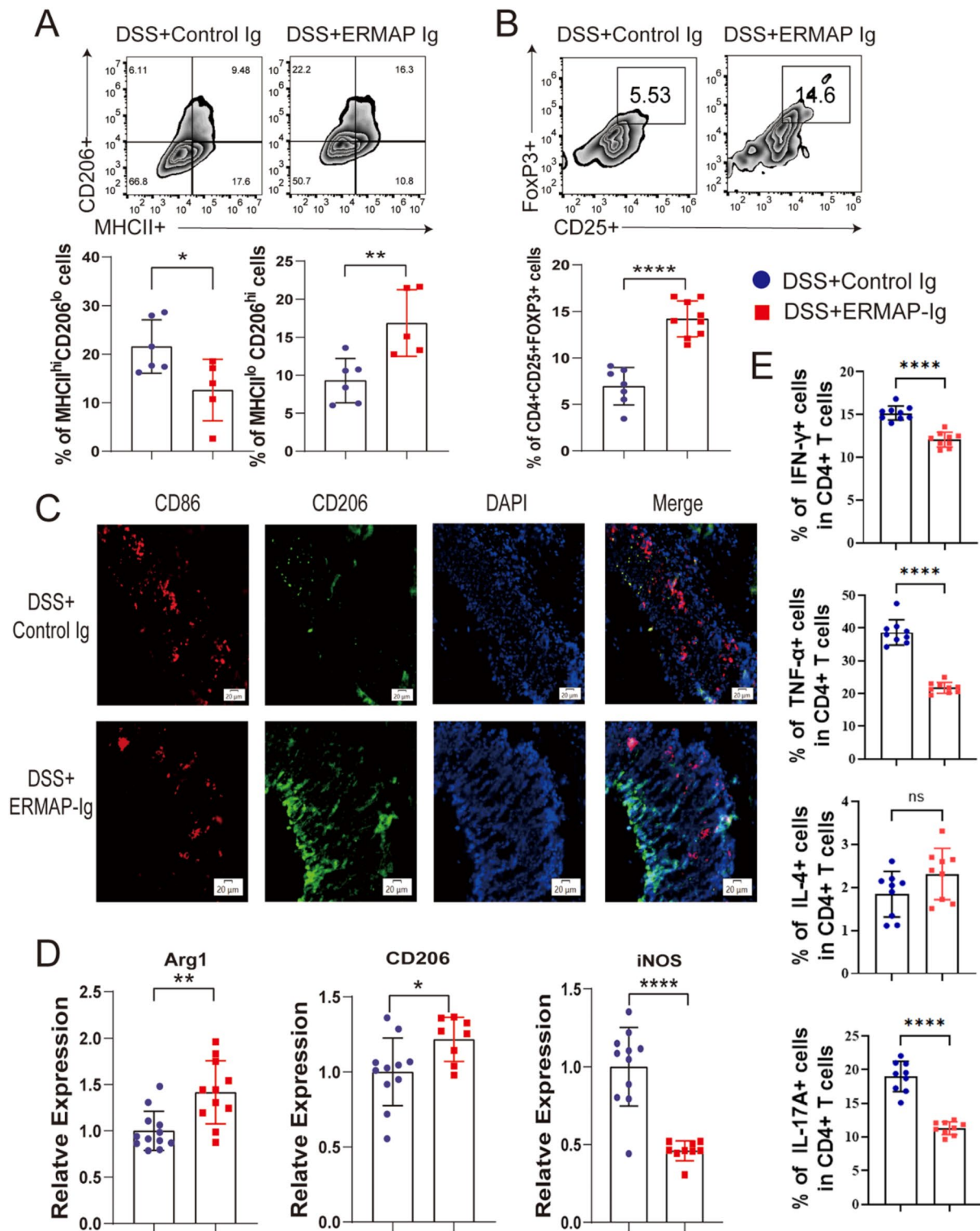


Fig. 2 ERMAP-Ig increases the number of intestinal M2 type macrophages in IBD mice. Flow cytometric analysis of colonic lamina cells of control Ig and ERMAP-Ig-treated DSS-induced colitis mice. **(A)** The percentages of MHCII^{hi}CD206^{lo} M1 and MHCII^{lo}CD206^{hi} M2 cells in F4/80⁺ cells. **(B)** The proportion of CD4⁺CD25⁺Foxp3⁺Tregs. **(C)** Colonic tissue sections were stained with anti-CD86 (red) and anti-CD206 (green) antibodies and observed under a microscope. **(D)** The mRNA expression levels of Arg1, CD206 and iNOS were measured in colon tissues by qRT-PCR. The expression level in control Ig-treated mice was defined as 1. **(E)** Flow analysis of inflammatory factor expression in CD4⁺ lymphocytes in colonic lamina cells. **P* < 0.05, ***P* < 0.01, *****P* < 0.0001 and ns compared with DSS + Control Ig

were increased in ERMAP-Ig mice. Given the observed effect of ERMAP-Ig on the number and differentiation of immune cells in DSS-induced colitis mice, we hypothesized that its therapeutic effects involve modulation of macrophage polarization and T cell responses.

Effects of ERMAP-Ig on T cell responses and macrophage polarization in DSS-induced colitis mice

We then examined T cell activation in the spleen by analyzing the expression of CD69, an activation marker. ERMAP-Ig treatment significantly decreased the percentages of CD69⁺ cells in CD4⁺ and CD8⁺ T cells (Fig. 3A), suggesting that ERMAP reduces T cell activation in DSS-induced colitis mice [2, 27]. We also determined T cell proliferation by analyzing CFSE dilution and Ki67⁺ cells. After 3 days of culture in pre-coated anti-CD3 (5 µg/mL) plates, CFSE dilution assay showed that the percentage of proliferative CD4⁺ T cells from ERMAP-Ig-treated mice was lower than that from control Ig-treated mice (Fig. 3B), which was confirmed by reduced percentage of Ki67⁺ CD4⁺ cells (Fig. 3C). Reduced Ki67⁺ CD8⁺ cells were also detected in ERMAP-Ig-treated mice (Fig. 3C). The results suggest that ERMAP inhibits T cell proliferation in DSS-induced colitis mice. Furthermore, ERMAP-Ig treatment increased the percentage of Tregs in the spleen (Fig. 3D). We also examined cytokines secreted by T cell subsets, and ERMAP-Ig increased IL-4 secretion by CD4⁺ T cells, and decreased TNF-α, IFN-γ, as well as IL-17 A secretion in the spleen (Supplemental Fig. 6). ERMAP-Ig also increased the percentage of MHCII^{lo} CD206^{hi} M2 macrophages but decreased the percentage of MHCII^{hi} CD206^{lo} M1 macrophages in F4/80⁺ cells (Fig. 3E). In addition, the percentage of TNF-α⁺ cell in F4/80⁺ macrophages were reduced in ERMAP-Ig-treated DSS-induced colitis mice (Fig. 3F). The results suggest that ERMAP-Ig treatment affects macrophage polarization.

Knockdown of ERMAP in RAW264.7 inhibits M2-type macrophage polarization and increases T cell responses

Since the macrophage line RAW264.7 express ERMAP protein (Supplemental Fig. 3), we determined the role of endogenous ERMAP on macrophage polarization and T cell response. RAW264.7 cells were transduced by lentivirus containing ERMAP-specific or control shRNA. The knockdown of ERMAP in the cells was confirmed by qRT-PCR, Western blot and flow cytometry, showing that the expression levels of the gene and protein in ERMAP-specific shRNA-treated cells were lower than those in control shRNA-treated cells (Supplemental Fig. 3). The cells were then induced to differentiate under the M1 or M2 condition. ERMAP knockdown increased MHCII^{hi} CD206^{lo} M1 macrophages under the M1 differentiation condition, but decreased MHCII^{lo}

CD206^{hi} M2 macrophages under the M2 differentiation condition (Fig. 4A). The results suggest that endogenous ERMAP inhibits M1 differentiation but promotes M2 differentiation.

To investigate the effect of macrophage ERMAP expression on T cells, the ERMAP shRNA or control treated RAW264.7 cells were co-cultured with splenocytes from C57BL/6 mice for 16 h. T cell activation and proliferation were then analyzed by flow cytometry. Co-culture with ERMAP knockdown macrophages increased the percentages of CD69⁺ CD4⁺ and CD8⁺ activated T cells as compared with co-culture with control treated macrophages (Fig. 4B). The percentage of proliferative Ki67⁺ cells in CD4 and CD8 T cells were also increased after co-culture with ERMAP knockdown macrophages (Fig. 4C). This is consistent with the data that ERMAP inhibits T cell activation and proliferation.

ERMAP-Ig reduced macrophage-mediated inflammation

We analyzed global gene expression between control shRNA and ERMAP shRNA-treated RAW264.7 macrophages by RNA-seq. A total of 131 genes were up-regulated and 14 genes were down-regulated in ERMAP shRNA-treated RAW264.7 macrophages (Supplementary Fig. 7). The cluster Profiler software was used to analyze the GO function enrichment of the differential gene set. The most significant 30 terms were selected to draw a bubble chart for display. The ordinate is the functional description corresponding to the GO number. The abscissa is the ratio of the number of differential genes annotated to the GO number to the total number of differential genes. The size of the dot represents the number of genes annotated on the GO Term, and the color from red to purple represents the significance of the enrichment (Fig. 5A).

We found the expression levels of several pathways in ERMAP shRNA-treated RAW264.7 cells as compared with control shRNA-treated cells were altered, including NOD-like receptor signaling pathway, RIG-I-like receptor signaling pathway, Toll-like receptor signaling pathway, and Cell adhesion molecules (CAMs). Among them, the number of differential genes related to NOD-like receptor signaling pathway was the largest. The NOD-like receptor (NLR) protein family is a group of pattern recognition receptors (PRRs) known to mediate the initial innate immune response to cellular damage and stress. NLRP3 is mainly present in macrophages and dendritic cells, and signals from inflammasome formation through classical Caspase-1 activation [28]. The mRNA expression levels of NLRP3, GSDMD, Caspase-1 and IL-1β in ERMAP shRNA RAW264.7 macrophages activated by LPS were significantly increased compared with those in control RAW264.7 macrophages (Fig. 5B),

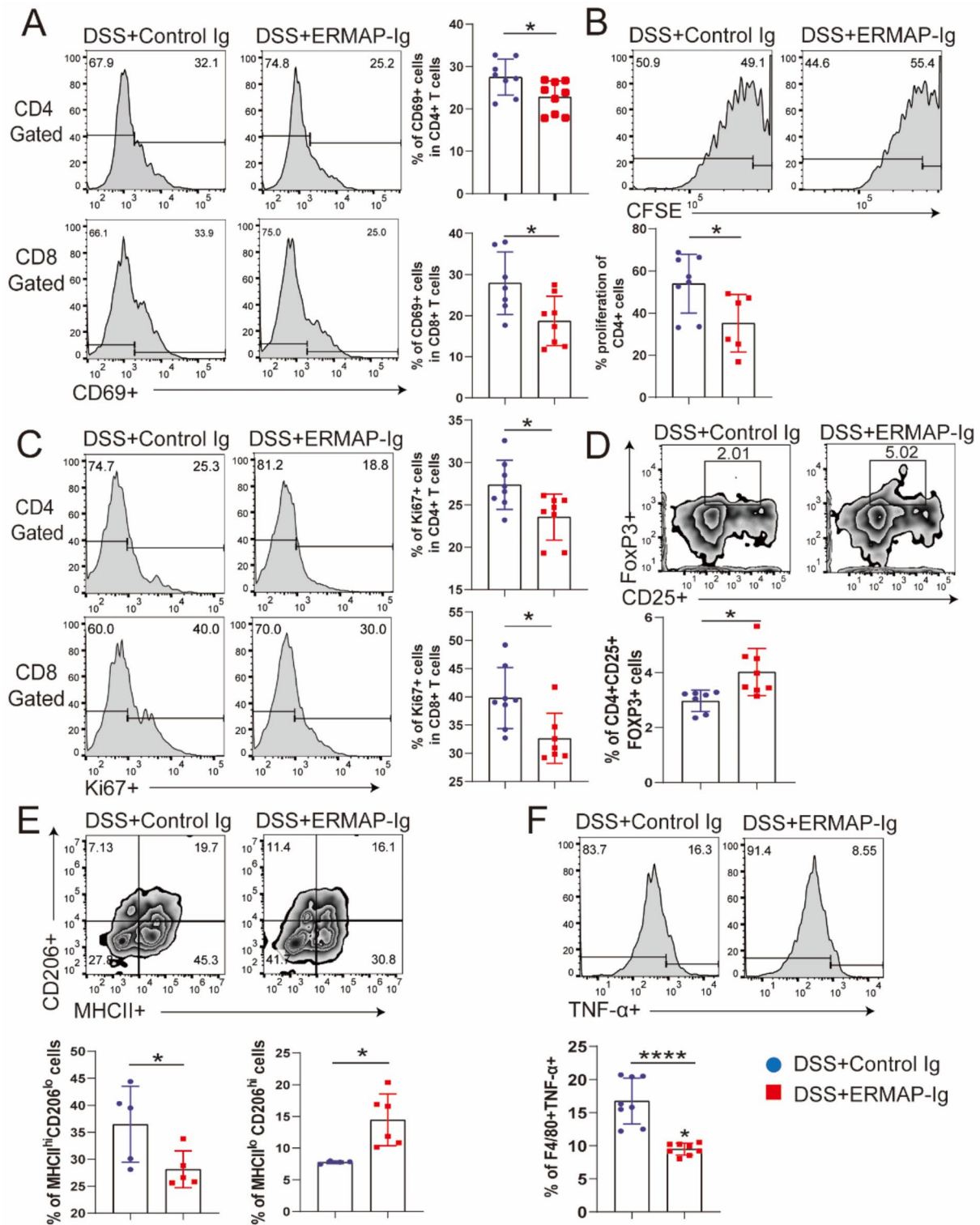


Fig. 3 Effects of ERMAP-Ig on T cell response and macrophage polarization in DSS-induced colitis. C57BL/6 mice were induced to develop DSS-induced colitis and treated with ERMAP-Ig or Control Ig as in Fig. 1. The spleens were collected on day 12. **(A)** FACS analysis for the expression of CD69 on CD4⁺ and CD8⁺ T cells. **(B)** CD4⁺ and CD8⁺ T cell proliferation was determined by **(B)** CFSE dilution assay and **(C)** Ki67 staining. **(D)** The percentages of CD4⁺ CD25⁺ Foxp3⁺ Tregs. **(E-F)** The percentages of M 1/ M2 and TNF-α⁺ cells in F4/80⁺ macrophages. This data is presented as the mean ± SD and represents three independent experiments with similar results. **P* < 0.05, *****P* < 0.0001 compared with DSS + Control Ig

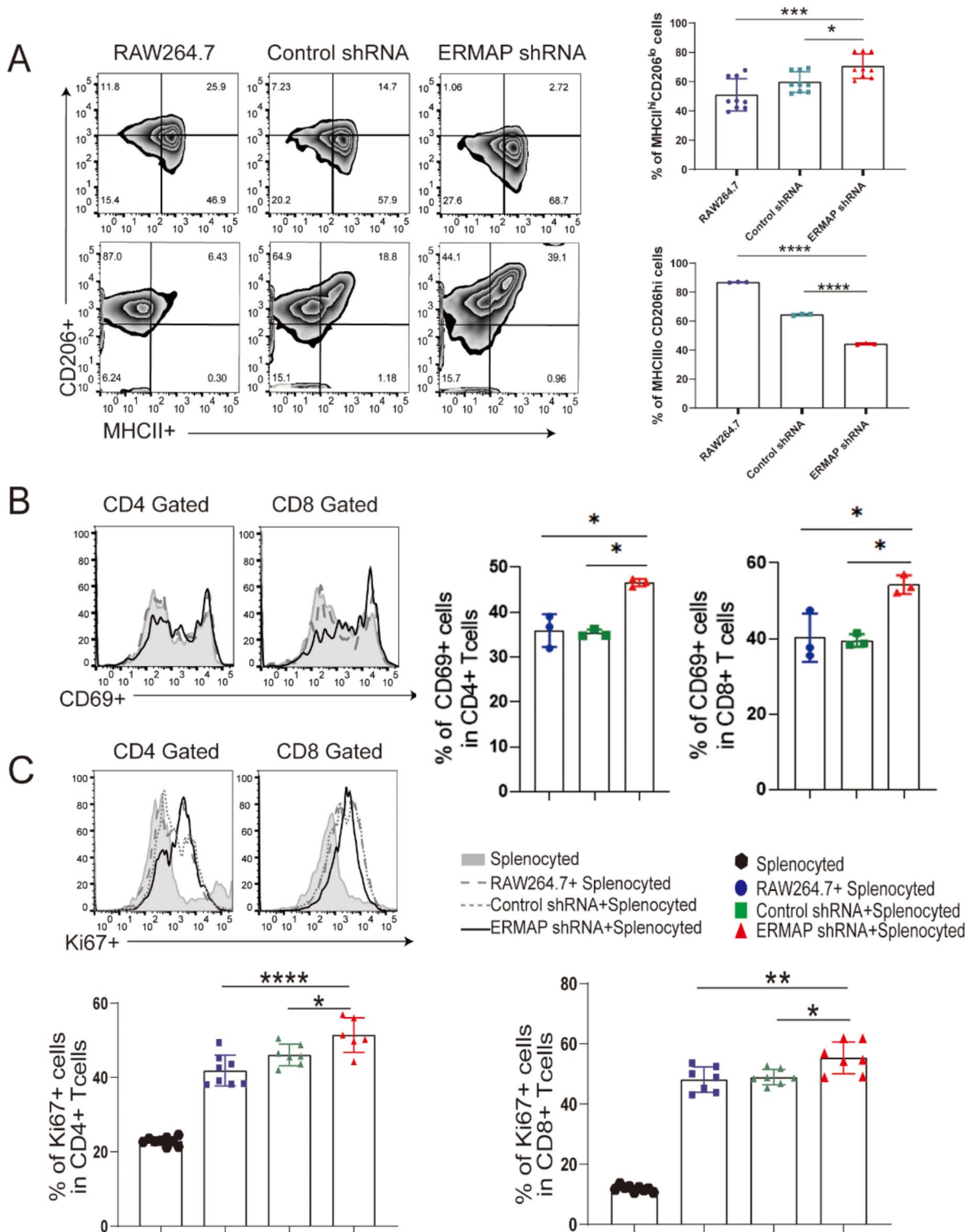


Fig. 4 Knockdown of ERMAP in RAW264.7 macrophages inhibits M2-type macrophage polarization and increases T cell responses. RAW264.7 macrophages were transfected with lentivirus containing ERMAP specific shRNA or control shRNA for 24 h. (A) The cells were induced to differentiate under M1 condition (LPS 100 ng/mL, IFN- γ 2.5 ng/mL) and M2 condition (IL-4 40 ng/mL). The proportion of MHCII⁺ CD206^{lo} M1 and MHCII^{lo} CD206^{hi} M2 were analyzed by flow cytometry. (B-C) Splenocytes of C57BL/6 mice were co-cultured with the ERMAP specific shRNA or control shRNA-treated RAW264.7 macrophages. Cells were then analyzed for the percentages of (B) CD69⁺ activated CD4⁺ and CD8⁺ T cells and (C) proliferative Ki67⁺ cells in CD4⁺ and CD8⁺ T cells that had been cultured in pre-coated anti-CD3 (5 μ g/mL) plates. * P < 0.05, ** P < 0.01, *** P < 0.001, **** P < 0.0001 vs. untreated RAW264.7 macrophages and/or control shRNA treated macrophages. The data are representative of three independent experiments with similar results

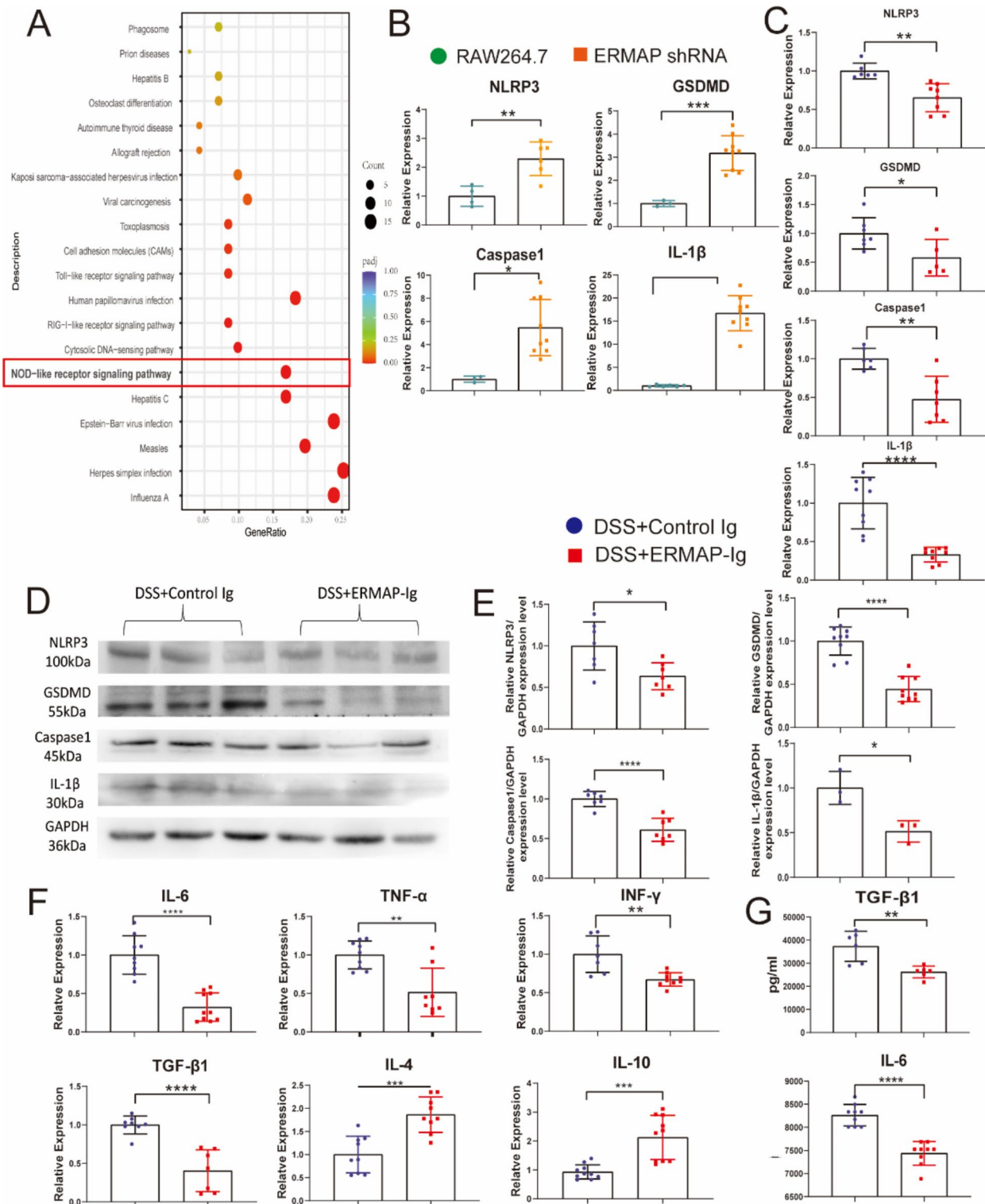


Fig. 5 ERMAP-Ig reduced macrophage-mediated inflammation. **(A)** Global gene expression between RAW264.7 with control shRNA and ERMAP shRNA treated RAW264.7 cells analyzed by RNA-seq, showing enrichment analysis of KEGG signaling pathway bubble diagram. **(B)** Control RAW264.7 and ERMAP shRNA RAW264.7 were stimulated by LPS for 24 h and then analyzed for the expression levels of the NOD-like receptor pathway-related genes by qRT-PCR. **(C)** qRT-PCR and **(D-E)** Western blot analyses for the expression levels of NOD-like receptor pathway-related genes and proteins in the colon tissue between Control Ig and ERMAP-Ig-treated IBD mice. **(F)** The expression levels of cytokines IL-1β, IL-6, TNF-α, TGF-β1, IL-4, IL-10 in the colon tissues between control Ig and ERMAP-Ig-treated IBD mice were determined by qRT-PCR. **(G)** The contents of TGF-β1 and IL-6 in the serum between control Ig and ERMAP-Ig-treated IBD mice were measured by ELISA. Experiments were repeated at least three times with * $P < 0.05$, ** $P < 0.01$, *** $P < 0.001$, **** $P < 0.0001$ vs. control cells or control Ig treated mice

suggesting these genes are the downstream targets and inhibited by ERMAP.

To confirm that NLRP3, GSDMD, Caspase-1, and IL-1 β are inhibited by ERMAP, we analyzed the expression of these genes between control Ig and ERMAP-Ig-treated DSS-induced colitis mice. The expression levels of all these genes in the ERMAP-Ig-treated mice were lower than those in control Ig-treated mice (Fig. 5C), which were also confirmed at protein level as analyzed by western blot (Fig. 5D-E).

We also detected the expression levels of cytokine mRNA in the colon. The relative mRNA expression of inflammatory cytokines IL-6, TNF- α , IFN- γ and TGF- β was significantly decreased, while the relative mRNA expression of inflammatory suppressor IL-4 and IL-10 was significantly increased in the ERMAP-Ig-treated DSS-induced colitis mice (Fig. 5F). Serum contents of TGF- β and IL-6 in the ERMAP-Ig-treated mice were also lower than those in the control Ig-treated mice (Fig. 5G). The results suggest that the effect that ERMAP-Ig alleviates the inflammatory response in DSS-induced colitis is likely related to the GSDMD inflammasome-associated signaling pathways.

ERMAP^{-/-} macrophages exacerbate DSS-induced colitis in WT mice

To confirm that ERMAP on macrophages play a protective role in DSS-induced colitis, we depleted macrophages (M ϕ) from WT mice using liposome-encapsulated clodronate, followed by transfer of WT or ERMAP^{-/-} (KO) peritoneal macrophages (Fig. 6A). Mice given ERMAP^{-/-} macrophages significantly increased their DAI scores from days 7 to 10 (Fig. 6B), and had more severe colon shortening (Fig. 6C-D) and body weight loss (Fig. 6F). Histological analysis revealed that mice given ERMAP^{-/-} macrophages had increased colonic damage (Fig. 6E).

The flow cytometric analysis showed that mice given ERMAP^{-/-} macrophages had fewer Tregs (Fig. 6G). In addition, both splenic T cell activation and proliferation in mice given ERMAP^{-/-} macrophages were increased (Fig. 6H-I). Analysis of the mRNA expression of inflammatory cytokines from the colon revealed that mice given ERMAP^{-/-} macrophages expressed more than given WT macrophages (Supplementary Fig. 8). Collectively, the results suggest that adoptively transfer of ERMAP^{-/-} macrophages promote the proliferation and activation of T cells and ERMAP on macrophages play a protective role against DSS-induced colitis.

Discussion

Although the etiology of IBD is not fully understood, available evidence suggests that excessive immunity to normal flora leading to deregulation of the mucosal

immune system is an important pathogenesis of IBD [29]. Anti-inflammatory drugs (glucocorticoid and amino-salicylic), immunosuppressant (azathioprine and methotrexate), and biological drugs (anti-TNF-drugs such as ustekinumab and Vedolizumab; The anti-p40 (IL-12 / 23) antibody ustekinumab) currently are the main drugs in IBD treatments [30]. However, these therapeutic approaches often have limited efficacy but severe adverse effects, calling for development of new therapies [31].

Increasing evidence has indicated that correct polarized state of macrophages is very important for controlling intestinal inflammation and maintaining homeostasis [32]. Despite the predominance of colonic M1 macrophages in colitis, M2 macrophages have important roles in antagonizing inflammation and promoting healing, which contributes to the resolution of inflammation [33]. Modulating the M1 / M2 polarization status of macrophages can alter the process of local inflammatory responses in the colon. Macrophage-targeted therapy is increasingly recognized as a novel treatment for intestinal inflammation [34].

Our previous studies have shown that ERMAP not only inhibits T cell functions, but also affect macrophage polarization [18]. In this study, we show that ERMAP-Ig treatment increases the number of M2 macrophages in the colon and spleen, decreases the mRNA levels of the pro-inflammatory cytokines TNF- α , IL-1 β , IL-6, IFN- γ and TGF- β 1, increases the mRNA expression of the inflammatory suppressors IL-4 and IL-10, and significantly improves inflammation and tissue damage in the colon. Consistent with the in vivo findings, the in vitro studies show that the ERMAP deletion increases the LPS-induced M1 polarization and reduces the IL-4-induced M2 polarization. Furthermore, adoptive transplantation of ERMAP^{-/-} peritoneal macrophages into DSS-induced colitis mice exacerbates inflammatory response and tissue damage. These results suggest that ERMAP affects macrophage polarization by generating more anti-inflammatory M2 macrophages, which plays an important role in the amelioration of DSS-induced colitis by ERMAP.

ERMAP also inhibits T cell activation, proliferation and inflammatory cytokine production, which are likely by the direct effects of ERMAP on T cells and indirect effects through increased production of M2 macrophages. Indeed, we have shown that T cells express the ERMAP receptor and ERMAP directly inhibits T cell functions in vitro [18]. In this study, we also show that co-culture T cells with ERMAP gene deleted macrophages increases the activation and proliferation of T cells. It is well known that CD4⁺ CD25⁺ Foxp3⁺ Tregs can prevent excessive inflammation [35]. ERMAP treatment increases the number of Tregs in DSS-induced colitis mice. The

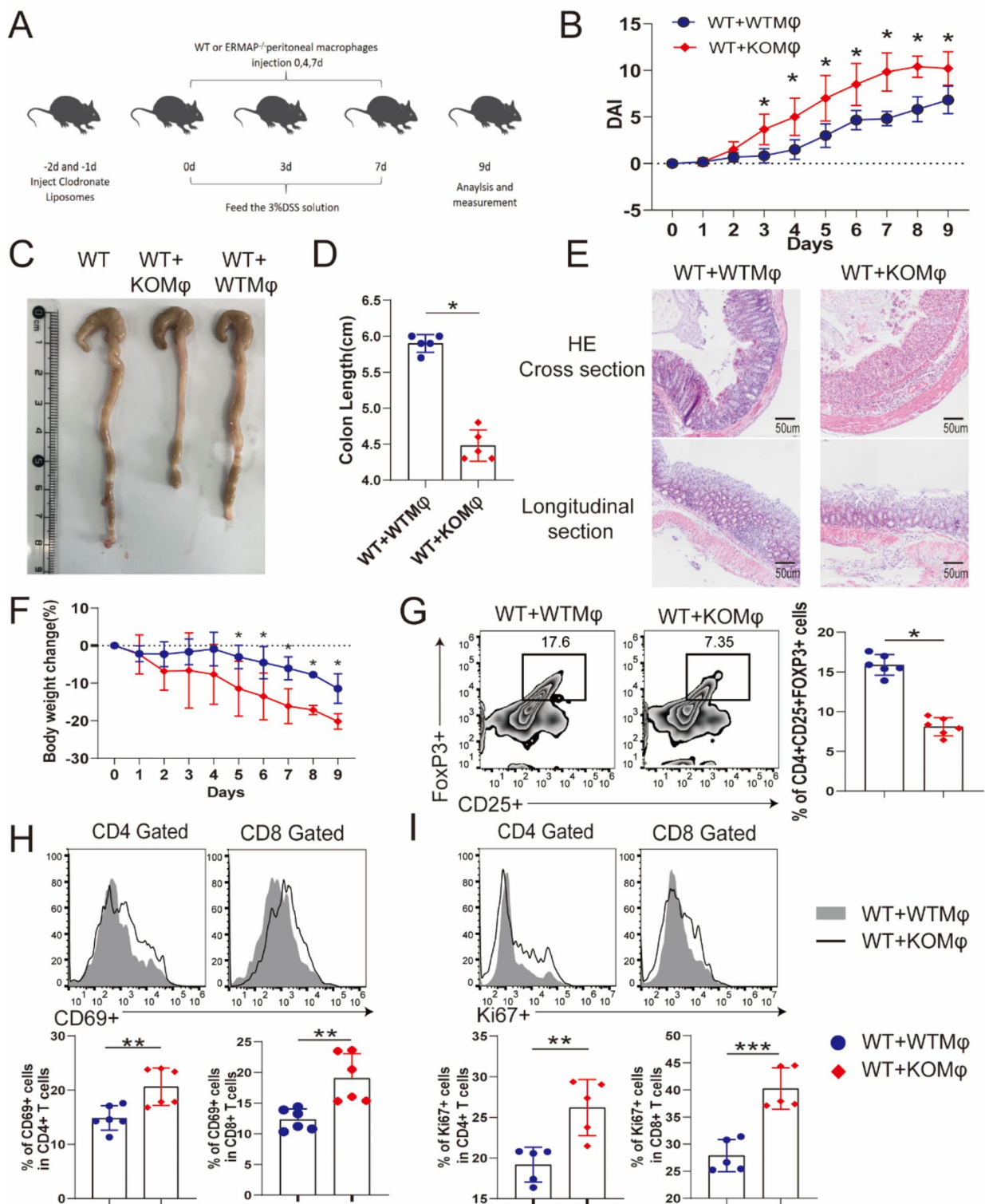


Fig. 6 ERMAP^{-/-} macrophages exacerbate DSS-induced colitis in WT mice. **(A)** Scheme of the macrophage adoptive transfer experiments. **(B)** Body weight and DAI scores of each group were measured daily (*n* = 6 for each group). **(C, D)** Colon's length was measured on day 9. **(C)** Typical images and **(D)** statistical analysis of the colon's length. **(E)** Representative histological images (200x) of the colon. **(F)** Body weight changes between the IBD mice that were transferred with WT or KO macrophages (*n* = 6 for each group). **(G)** The percentages of CD4⁺ CD25⁺ Foxp3⁺ Tregs. **(H)** The expression of CD69 on CD4⁺ and CD8⁺ T cells in spleen cells, **(I)** The percentage of Ki67⁺ proliferative cells in CD4 and CD8 T cells. **P* < 0.05, ***P* < 0.01, ****P* < 0.001, *****P* < 0.0001 compared with WT + WT Mφ. The data are representative of two independent experiments with similar results

underlying mechanisms could also be due to direct and / or indirect effects of ERMAP on Tregs [36].

IBD represents an imbalance in the intestinal immune response. Recent studies have shown that excessive worsening of pyroptosis plays a key role in the development of autoimmune diseases [37]. Pyroptosis is characterized by pore formation in the cell membrane, cell rupture, and the excretion of cellular contents and pro-inflammatory cytokines, such as IL-1 β and IL-18. This hyperactive inflammatory programmed cell death disrupts the homeostasis of the immune system and promotes autoimmunity [38]. The NLRP3 inflammasome is highly expressed in patients with autoimmune diseases, and the NLRP3 axis readily triggers immune system over-response through the classical caspase1- dependent pathway / IL-1 β axis [39]. Our RNA-seq analysis shows that the key genes in the NLRP3 axis were increased in ERMAP gene deleted macrophages. In contrast, ERMAP-Ig administration significantly reduced the expression of NLRP3 axis genes in the colon of DSS-induced colitis mice. Our results suggest that the NLRP3 axis may play a key role in the effects of ERMAP on macrophages.

In summary, our results suggest that administration of ERMAP can protect DSS-induced colitis in mice by regulating T cell and macrophage functions. This study adds to the evidence for various mechanistic pathways associated to the pathogenesis of IBD, which could subsequently be translated to novel therapeutics.

Abbreviations

IBD	Inflammatory bowel disease
ERMAP	Erythrocyte Membrane-associated Protein
DSS	Dextran sodium sulfate
Control Ig	Control Fc protein
ERMAP-Ig	ERMAP-Fc fusion protein
DAI	Disease activity index
ERMAP ^{-/-}	ERMAP knockout mice
NLR	NOD-like receptor
GI	Gastrointestinal
PAMPs	Pathogen-associated molecular patterns
DAMPs	Damage-associated molecular patterns
M1	Classically activated macrophages
M2	Selectively activated macrophages
LPS	Lipopolysaccharide
Arg 1	Arginase I
EAE	Experimental autoimmune encephalomyelitis
T1D	Type I diabetes mellitus
WT	Wild-type
Tregs	Regulatory T cells
i.p.	Intraperitoneally
ATCC	American type culture collection
DMEM	Dulbecco's modified Eagle's medium
FBS	Fetal bovine serum
CAMs	Cell adhesion molecules
PRRs	Pattern recognition receptors

Supplementary Information

The online version contains supplementary material available at <https://doi.org/10.1186/s12876-025-03840-z>.

Supplementary Material 1

Acknowledgements

None declared.

Author contributions

L.X., Y.P.; investigation, methodology, writing-original draft; X.W.: data curation; R.H.: Conceptualization, Project administration, Data curation, Writing - review & editing; J.G.: Investigation; W.C.: Investigation; K.H.: Investigation; D.C.: Investigation; Y.Z.: Methodology, Formal analysis; L.L.: Conceptualization, Formal analysis; L.L.: Conceptualization; Writing - review & editing; M.S.: Conceptualization, Funding acquisition, Project administration, Methodology, Writing - review & editing.

Funding

This work was supported by the National Natural Science Foundation of China to Min Su (82171343 and 82060151) and by the Science and Technology Foundation of Guizhou Province to Min Su (Qiankehezhicheng [2020]4Y230 and Qiankeherencaipingtai [2020]4103) and to Youbo Zhao (Qiankehejichu-zk [2022]-404). This work was also supported by the project for Key Laboratory of Higher Education schools in Guizhou Province (Qianjiaoji [2023]016) to Min Su.

Data availability

Data is provided within the manuscript or supplementary information files.

Declarations

Ethics approval and consent to participate

This work was approved by the Institutional Animal Care and Use Committee of Guizhou Medical University (NO: 1900035). This study did not conduct any experiments on human subjects, so written informed consent from participants was not required.

Consent for publication

Not applicable.

Competing interests

The authors declare no competing interests.

Author details

¹Center for Tissue Engineering and Stem Cell Research, Guizhou Medical University, 6 Ankang Avenue, Gui'an New District, Guizhou 561113, China

²Department of Histology and Embryology, Guizhou Medical University, 6 Ankang Avenue, Gui'an New District, Guizhou 561113, China

³Key Laboratory for Research on Autoimmune Diseases of Higher Education schools in Guizhou Province, 6 Ankang Avenue, Gui'an New District, Guizhou 561113, China

⁴Translational Medicine Research Center of Guizhou Medical University, 6 Ankang Avenue, Gui'an New District, Guizhou 561113, China

⁵The Public Health Clinical Center of Guiyang City, 6 Daying Road, Guiyang City 550004, Guizhou, China

⁶Department of Allied Health Sciences, University of Connecticut, 1390 Storrs Road, Storrs, CT 06269, USA

⁷Key Laboratory of Adult Stem Cell Translational Research (Chinese Academy of Medical Sciences), Guizhou Medical University, 6 Ankang Avenue, Gui'an New District, Guizhou 561113, China

Received: 29 October 2024 / Accepted: 2 April 2025

Published online: 12 May 2025

References

1. Nakase H, Uchino M, Shinzaki S, et al. Evidence-based clinical practice guidelines for inflammatory bowel disease 2020. *J Gastroenterol.* 2021;56:489–526.
2. Yasutomi Y, Chiba A, Haga K, et al. Activated Mucosal-associated invariant T cells have a pathogenic role in a murine model of inflammatory bowel disease. *Cell Mol Gastroenterol Hepatol.* 2022;13:81–93.

3. Bain CC, Bravo-Blas A, Scott CL, et al. Constant replenishment from circulating monocytes maintains the macrophage pool in the intestine of adult mice. *Nat Immunol*. 2014;15:929–37.
4. Muller PA, Matheis F, Mucida D. Gut macrophages: key players in intestinal immunity and tissue physiology. *Curr Opin Immunol*. 2020;62:54–61.
5. Leal MC, Dabritz J. Immunoregulatory role of Myeloid-derived cells in inflammatory bowel disease. *Inflamm Bowel Dis*. 2015;21:2936–47.
6. Dheer R, Davies JM, Quintero MA, et al. Microbial signatures and innate immune gene expression in lamina propria phagocytes of inflammatory bowel disease patients. *Cell Mol Gastroenterol Hepatol*. 2020;9:387–402.
7. Mosser DM, Edwards JP. Exploring the full spectrum of macrophage activation. *Nat Rev Immunol*. 2008;8:958–69.
8. Gordon S, Martinez FO. Alternative activation of macrophages: mechanism and functions. *Immunity*. 2010;32:593–604.
9. Ma S, Zhang J, Liu H, et al. The role of Tissue-Resident macrophages in the development and treatment of inflammatory bowel disease. *Front Cell Dev Biol*. 2022;10:896591.
10. Bain1 CC, 1 AMM. Macrophages in intestinal homeostasis and inflammation. *Immunol Rev*. 2014;260:102–17.
11. Sleiman J, Wei W, Shah R, et al. Incidence of immune checkpoint inhibitor-mediated diarrhea and colitis (imDC) in patients with cancer and preexisting inflammatory bowel disease: a propensity score-matched retrospective study. *J Immunother Cancer*. 2021;9:1–10.
12. Buhlmann JE, Elkin SK, Sharpe AH. A role for the B7-1/B7-2:CD28/CTLA-4 pathway during negative selection. *J Immunol*. 2003;170:5421–8.
13. Mace TA, Shakya R, Pitarresi JR, et al. IL-6 and PD-L1 antibody blockade combination therapy reduces tumour progression in murine models of pancreatic cancer. *Gut*. 2018;67:320–32.
14. Cui C, Su M, Lin Y, et al. A CD300c-Fc fusion protein inhibits T cell immunity. *Front Immunol*. 2018;9:2657.
15. Lin Y, Cui C, Su M, et al. Identification of TAPBPL as a novel negative regulator of T-cell function. *EMBO Mol Med*. 2021;13:e13404.
16. Wagner FF, Poole J, Flegel WA. Scianna antigens including Rd are expressed by ERMAP. *Blood*. 2003;101:752–7.
17. Liu H, Zhao J, Lin Y, et al. Administration of anti-ERMAP antibody ameliorates Alzheimer's disease in mice. *J Neuroinflammation*. 2021;18:268.
18. Su M, Lin Y, Cui C, et al. ERMAP is a B7 family-related molecule that negatively regulates T cell and macrophage responses. *Cell Mol Immunol*. 2021;18:1920–33.
19. Hunter MM, Wang A, Hirota CL, et al. Neutralizing anti-IL-10 antibody blocks the protective effect of tapeworm infection in a murine model of chemically induced colitis. *J Immunol*. 2005;174:7368–75.
20. You Y, Zhou C, Li D, et al. Sorting nexin 10 acting as a novel regulator of macrophage polarization mediates inflammatory response in experimental mouse colitis. *Sci Rep*. 2016;6:20630.
21. Mortazavi A, Williams BA, McCue K, et al. Mapping and quantifying mammalian transcriptomes by RNA-Seq. *Nat Methods*. 2008;5:621–8.
22. Liao Y, Smyth GK, Shi W. FeatureCounts: an efficient general purpose program for assigning sequence reads to genomic features. *Bioinformatics*. 2014;30:923–30.
23. Pineda-Torra I, Gage M, de Juan A, et al. Isolation, culture, and polarization of murine bone Marrow-derived and peritoneal macrophages. *Methods Mol Biol*. 2015;1339:101–9.
24. Geng J, Chen R, Yang FF, et al. CD98-induced CD147 signaling stabilizes the Foxp3 protein to maintain tissue homeostasis. *Cell Mol Immunol*. 2021;18:2618–31.
25. Leber A, Hontecillas R, Zoccoli-Rodriguez V, et al. Oral treatment with BT-11 ameliorates inflammatory bowel disease by enhancing regulatory T cell responses in the gut. *J Immunol*. 2019;202:2095–104.
26. Murai M, Turovskaya O, Kim G, et al. Interleukin 10 acts on regulatory T cells to maintain expression of the transcription factor Foxp3 and suppressive function in mice with colitis. *Nat Immunol*. 2009;10:1178–84.
27. Giuffrida F, Di Sabatino A. Targeting T cells in inflammatory bowel disease. *Pharmacol Res*. 2020;159:105040.
28. Wang Y, Zhou X, Zou K, et al. Monocarboxylate transporter 4 triggered cell pyroptosis to aggravate intestinal inflammation in inflammatory bowel disease. *Front Immunol*. 2021;12:644862.
29. Bourgonje AR, Roo-Brand G, Lisotto P, et al. Patients with inflammatory bowel disease show IgG immune responses towards specific intestinal bacterial genera. *Front Immunol*. 2022;13:842911.
30. Greuter T, Rieder F, Kucharzik T. Emerging treatment options for extraintestinal manifestations in IBD. *Gut*. 2021;70:796–802.
31. Both Dalm V, Richardson SA, et al. Inflammatory bowel disease in primary immunodeficiency disorders is a heterogeneous clinical entity requiring an individualized treatment strategy: A systematic review. *Autoimmun Rev*. 2021;20:102872.
32. Perez-Sanchez C, Barbera Betancourt A, Lyons PA, et al. miR-374a-5p regulates inflammatory genes and monocyte function in patients with inflammatory bowel disease. *J Exp Med*. 2022;219:1–16.
33. Bain CC, Mowat AM. Macrophages in intestinal homeostasis and inflammation. *Immunol Rev*. 2014;260:102–17.
34. Na YR, Stakenborg M, Seok SH, et al. Macrophages in intestinal inflammation and resolution: a potential therapeutic target in IBD. *Nat Rev Gastroenterol Hepatol*. 2019;16:531–43.
35. MacManus CF, Collins CB, Nguyen TT, et al. VEN-120, a Recombinant human lactoferrin, promotes a [Treg]ulatory [Treg] cell [Treg] phenotype and drives resolution of inflammation in distinct murine models of inflammatory bowel disease. *J Crohns Colitis*. 2017;11(9):1110–12.
36. Gentili M, Ronchetti S, Ricci E, et al. Selective CB2 inverse agonist JTE907 drives T cell differentiation towards a Treg cell phenotype and ameliorates inflammation in a mouse model of inflammatory bowel disease. *Pharmacol Res*. 2019;141:21–31.
37. You R, He X, Zeng Z, et al. Pyroptosis and its role in autoimmune disease: A potential therapeutic target. *Front Immunol*. 2022;13:841732.
38. Song Y, Zhao Y, Ma Y, et al. Biological functions of NLRP3 inflammasome: A therapeutic target in inflammatory bowel disease. *Cytokine Growth Factor Rev*. 2021;60:61–75.
39. Wang L, Crackower MA, Wu H. Advances toward structure-based drug discovery for inflammasome targets. *J Exp Med*. 2022;219:1–3.

Publisher's note

Springer Nature remains neutral with regard to jurisdictional claims in published maps and institutional affiliations.